A Numerical Study of Impingement Heat Transfer in a Confined Circular Jet

In Gyu Park*, Bock Choon Pak and Young I. Cho*****

(*Received July 8, 1996*)

Heat transfer characteristics of a submerged circular jet impingement with a confined plate was studied numerically. The continuity, momentum and energy equations were solved simultaneously. FIDAP, a finite element code, was used to formulate and solve the matrix equations for fluid elements. The effects of channel height and Reynolds number on the local Nusselt number were considered in the range of H=0.5-1.5 and Re=100-900, respectively. It was found that the channel height influenced strongly on the surface temperature, shear stress and pressure drop. The peak temperature was observed and gradually moved outward to the rim of the heated circular plate with increasing the Reynolds number, which may be related to flow recirculation region in the channel. It is also noted that the pressure drop increased more than the average heat transfer coefficient as the Reynolds number increased. For Pr=7, the Nusselt number was much more dependent on the Reynolds number than the channel height, and the magnitude of the second peak in the Nusselt number distribution increased as the Reynolds number increased. The local Nusselt number calculated based on a mixing-cup temperature was considerably different from that using the inlet nozzle temperature for H=0.5 and Re=100. The present study showed that the local Nusselt number of a confined submerged jet was significantly larger than that of the unconfined free jet which was available in the literature.

Key Words: Impingement Heat Transfer, Submerged Confined Jet, Channel Height

Nomenclature

A : Heated plate area
C_p : Specific heat at constant pressure
d : Inner diameter of the nozzle ($=2r_0$)
h : Local heat transfer coefficient
$\bar{h}$: Average heat transfer coefficient
H : Dimensionless channel height, $H=Z/r_0$
k : Thermal conductivity
Nu : Local Nusselt number, hd/k
$\overline{Nu}_T$: Average Nusselt number, defined as Eq. (1)
$\overline{Nu}_h$: Average Nusselt number, defined as Eq. (2)
p : Pressure
Δp : Pressure drop
Pr : Prandtl number
q : Heat flux at the heated plate wall, constant
r : Radial coordinate
Re : Reynolds number, defined as $\rho V_{in} d/\mu$
T : Temperature
$\bar{T}$: Average bottom plate temperature
V : Velocity
$\bar{V}$: Average velocity at jet-to-plate spacing
z : Axial coordinate
Z : Channel height

Greek Letters

μ : Viscosity
ρ : Density
τ : Local shear stress

Subscripts

in : Nozzle inlet

*Mando Machinery Co., Asan Plant, Asan, Chungnam, 337-840, Korea
**School of Mech. Eng., Chonbuk National Univ., Chonju, Chonbuk 560-756, Korea
***Dept. of Mech. Eng. and Mechanics, Drexel University, Philadelphia, 19104 PA, U. S. A.

mix : Mixing-cup
w : Wall

1. Introduction

Impingement jet is of great practical interest since it can be used as an effective means of providing high heat transfer rates in various industrial transport processes. Some industrial applications include thermal treatment in annealing process of metals, drying of textiles and paper, cooling of internal combustion engines, and more recently, thermal control of the high-heat-dissipation electronic components.

Impingement jets can be primarily categorized into two broad groups : (i) gas jets ; (ii) liquid jets by the type of working fluid. Also, it can be classified into free or submerged jets depending on flow situation, and besides into the unconfined and confined cases depending on whether a confinment plate exists or not.

A tremendous amount of technical papers dealing gas and liquid jets and recent reviews (Downs and James, 1987 ; Webb and Ma, 1995) on that subject exist in the literature. However, limited information is available for the effect of the confined or partially confined plates on impinging jet flow and heat transfer characteristics. Furthermore, no previous studies of an axisymmetric liquid jet impingement in the laminar flow, particularly for the confined submerged case, has been reported. Much useful information can be found in closely related studies as summaried in the following.

For an axisymmetric jet impingement with a circular nozzle, both the free and submerged cases were studied by Womac et al. (1993). The unconfined submerged jet impingement was investigated by Deshpande and Vaishnav (1982), Ma and Bergles (1983), Sparrow et al. (1987), and Womac et al(1993). Ma and Bergles (1983) experimentally studied heat removal from the electrically heated chip-size test sections with normally impinging circular submerged jets of R-113 fluid. They found that high heat flux rate of approximately 20 watts/chip could be obtained with a subcooled R-113 jet impingement. Womac et al. (1993) found that the average Nusselt number ($\overline{Nu}_T$) of a submerged jet for $Re \leq 4000$ was lower than under that of a free jet. For $H \leq 8$, the average Nusselt number ($\overline{Nu}_T$) was insensitive to the channel heights. However, for $H > 8$, it relatively decreased with increasing channel heights.

A confined submerged jet impingement in laminar flow was numerically studied by Saad et al. (1977). They reported that the characteristics of impinging round jets depended on the inlet jet velocity profile (i. e., whether it is a flat or parabolic velocity profile). For the flat inlet velocity profile, the heat transfer rate was significantly less along the entire impingement plate than for the parabolic velocity profile. Although test conditions for Sadd et al. (1977) were similar to the present numerical study, their results were not suitable for comparison because the Prandtl number for air (0.7) in their study was different from that (≈ 7) of the present study by one order of magnitude.

Inada et al. (1981) conducted a theoretical and experimental study of the unconfined impinging jet on the laminar-flow heat transfer with constant heat flux at the wall. They found that the heat transfer coefficients reached a peak value at the stagnation point (i. e., at the center of disk) for dimensionless channel height $H = 1.4$ and at the point of about half rectangular slot width from the stagnation point for $H = 0.2 - 0.5$.

Stevens and Webb (1991) investigated the local heat transfer coefficients for round, single-phase free liquid jets impinging normally against a flat plate with constant heat flux. They reported that the nozzle diameter instead of the channel height was a major parameter in determination of the local heat transfer coefficient. They also found that beyond dimensionless distance $r/r_0 = 1.5$, the local Nusselt number profile exhibited a sharp drop followed by gradual decrease. In some cases, a second peak in the Nusselt number occurred after this gradual decrease when the Reynold number increased.

In the present study, a confined submerged liquid jet was examined in the laminar flow with impinging outflow passing beyond the outer rim

of a heated surface. The objective of the present study was to investigate the effect of the channel height and the magnitude of velocity on temperature profile, shear stress, and local Nusselt number.

2. Numerical Modelling

A submerged confined radial jet impingement as shown in Fig. 1 schematically was considered for the present numerical simulation. Axisymmetric, two-dimensional, steady flow with constant heat flux boundary condition was assumed. A circular nozzle of the inner diameter of 1 cm was located at the center of the top surface. The working fluid was assumed to be water at 20℃ of which the density and viscosity are 0.9982 g/cm^3 and 1.002 mPa. s, respectively.

To investigate the effect of the channel height on heat transfer characteristics, three different dimensionless channel heights (H=0.5, 1.0 and 1.5) were used. Also, three different Reynolds numbers of 100, 500 and 900 were used for each channel height in order to examine the effect of the Reynolds number.

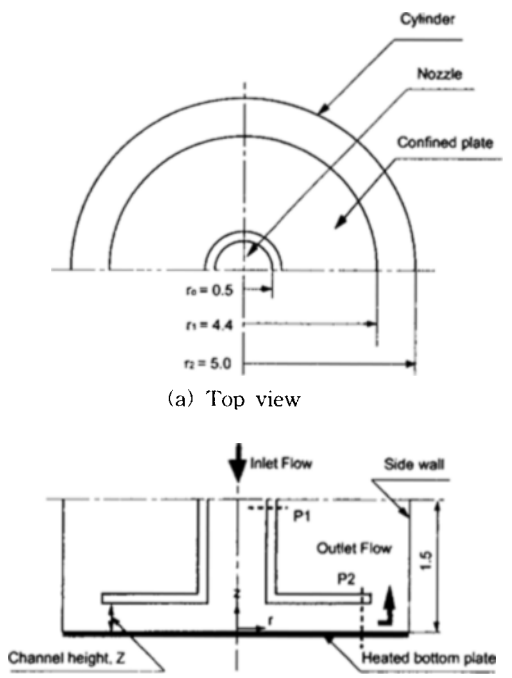

Fig. 1 Schematic diagram of a liquid jet cooling module for the automobile engine head. All dimensions are given in [cm]

The continuity, momentum and energy equations were solved simultaneously. The governing equations used in the present numerical study are presented in vector forms as follows :

Continuity equation

$$\nabla \cdot \boldsymbol{u} = 0 \tag{1}$$

Momentum equation

$$\rho \boldsymbol{u} \cdot \nabla \boldsymbol{u} = -\nabla p + \mu \nabla^2 \boldsymbol{u} \tag{2}$$

Energy equation

$$\rho C_P \boldsymbol{u} \cdot \nabla T = k \nabla^2 T \tag{3}$$

where the viscous dissipation and buoyancy terms were assumed to be negligible. Adiabatic walls were assumed at the confined plate and the side wall of a cylinder (see Fig. 1).

FIDAP, a commercial finite element code, was used to formulate and solve the matrix equations for fluid elements. Grids which were non-uniform for both z and r directions, consisted of a set of orthogonally intersecting straight lines with dense grids near the walls. For the case of H=0.5, grid of 47×115 was used; grid of 51×115 for H=1.0; grid of 57×115 for H=1.5, respectively. A quadratic boundary element (3 nodes) was used in the heat flux boundary condition, and a quadratic quadrilateral element (9 nodes) was used elsewhere. The number of iteration steps required for convergence was less than 10 ; only successive substitution method was used. For the final results of the present numerical computation, the solution procedures were repeated with the following convergence criteria for both the velocity and residual force norm :

$$\frac{\|u_i - u_{i-1}\|}{\|u_i\|} \leq 0.015 \tag{4}$$

and

$$\frac{\|R_i\|}{\|R_0\|} \leq 0.05 \tag{5}$$

where is the ith iteration solution vector and is the initial residual force vector. The iteration was terminated when these convergence criteria were satisfied simultaneously.

The two average Nusselt numbers over the

heated bottom plate were determined from the following equations :

$$\overline{Nu}_T = \frac{q_w d}{k(\bar{T} - T_{in})} \tag{6}$$

and

$$\overline{Nu}_h = \frac{\bar{h} d}{k} \tag{7}$$

where $\bar{T}$ and $\bar{h}$ were calculated by the following equations :

$$\bar{T} = \frac{1}{A}\int T_w dA \tag{9}$$

$$\bar{h} = \frac{1}{A}\int h dA \tag{10}$$

where A is the bottom plate area and h is the local heat transfer coefficient, which is defined as

$$h = q_w/(T_w - T_{in}) \tag{11}$$

Also, the Reynolds number was defined as

$$Re = \rho V_{in} d/\mu \tag{12}$$

3. Results and Dicussion

3.1 Temperature variation on impingement surface

Figure 2 presents the results of the heated plate temperature vs. dimensionless radial distance at the different Reynolds numbers of 100, 500 and 900. At the low Reynolds number, the temperature increases monotonically regardless of the channel height, which is a typical temperature profile for impingement cooling reported in the previous literature. However, the peak point begins to be appeared in the intermediate flow region at the higher Reynolds number. Furtheremore, it moves out radially with increasing dimensionless channel height and the Reynolds number.

Since most axisymmetric submerged flow studies considered the dimensionless radial distance (r/r_0) less than 6 and dimensionless channel height (Z/r_0) greater than 3, it is hard to find data which can be compared with the present results. It is of note that the present data were obtained for the dimensionless distance of $0 < r/r_0 < 10$ and the dimensionless channel height of $0.5 < H < 1.5$ with a 180 degree turn in outflow (see

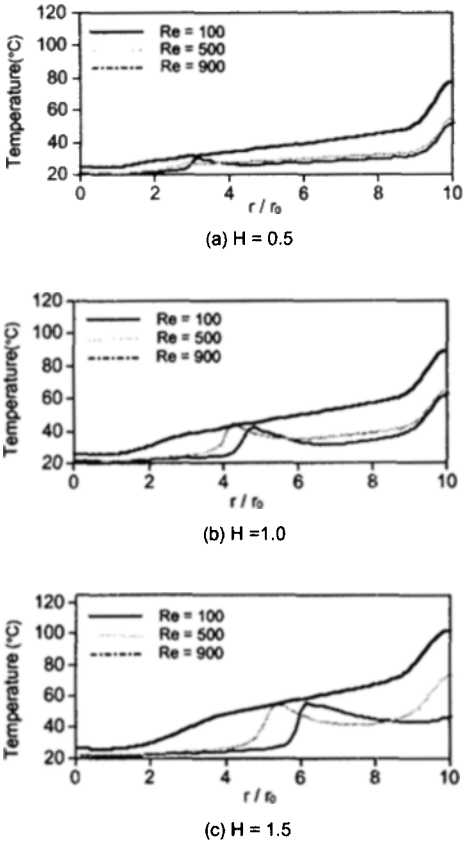

Fig. 2 Variation of the heated plate temperature along impingement surface at different Reynolds number

Fig. 1). In electronic packaging, compactness is an important requirement. Thus, the channel height should be minimized as much as possible. Many authors such as Sparrow et al. (1987), Womac et al. (1993) showed that the submerged jet data depended critically on the dimensionless channel height (H) more than the free surface jet data did.

Figure 3 shows the streamline plot and the corresponding temperature profile for $H = 1.5$ and $Re = 900$. The surface temperature of the heated bottom plate was maintained below 30℃ for $r/r_0 < 5.5$, which can be explained by the radial flow acceleration along the bottom plate due to the recirculation zone on the confined plate. At $r/r_0 \cong 6.0$, the surface temperature of the bottom plate suddenly increased to 57℃ caused by presence of the flow recirculation zone on the

heated bottom plate. Since this sudden increase can cause a locally hot spot, one must design flow impingement to avoid this flow recirculation zone on the bottom plate.

Figure 4 shows maximum surface temperatures as a function of Reynolds number at three different dimensionless heights. Two heated bottom areas were considered to select the maximum temperature in this figure. The solid line represents the maximum surface temperature in the overall area from the center to the rim of the bottom plate ($0<r\leq r_2$), and dashed line indicates the maximum surface temperature in the area occupied by the top confined plate ($0<r\leq r_1$). As shown in Fig. 6, the maximum surface temperatures were located mostly outside of the confined area. The maximum surface temperature decreased sharply when the Reynolds number increased from 100 to 500. The maximum temperature then gradually decreased as the Reynolds number further increased to 900.

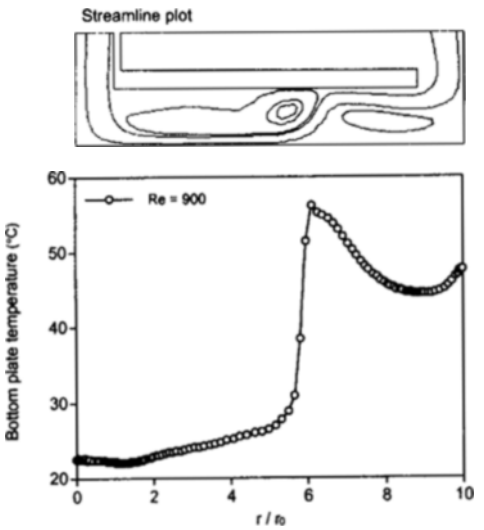

Fig. 3 Comparison of the heated plate temperature with streamline profile for $Re=900$ and $H=1.5$

3.2 Pressure effects to heat transfer

Figure 5 shows the relation between pressure drop and average heat transfer coefficient, whereas Fig. 6 shows the corresponding relation between the shear stress and local heat transfer coefficient. Figure 5(a) presents the pressure drop between the nozzle inlet, P_1 and the channel exit, P_2, (see the points P_1 and P_2 in Fig. 1) as a function of Reynolds number at three different

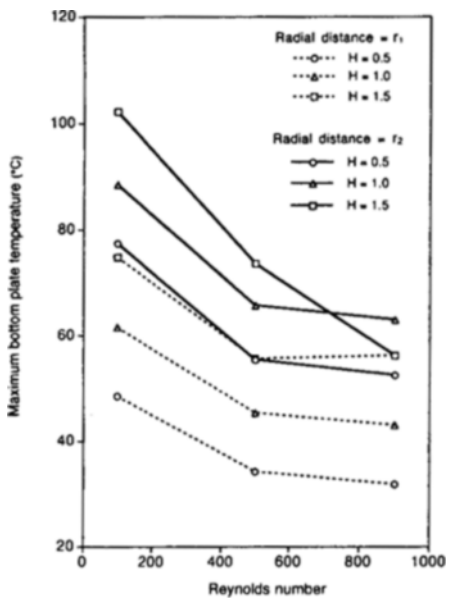

Fig. 4 Values of the local maximum heated plate temperature in the confined area ($0<r<r_1$) and overall area ($0<r<r_2$)

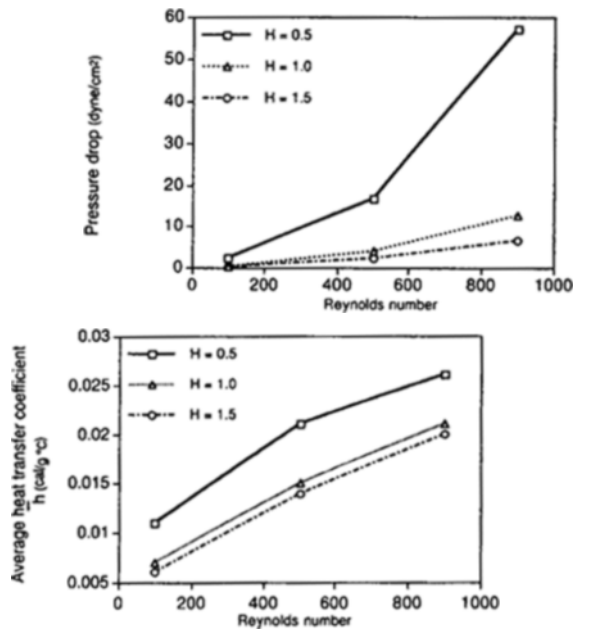

Fig. 5 Pressure drop and average heat transfer coefficient as a function of Reynolds number

dimensionless channel heights. Figure 5(b) shows the average heat transfer coefficient as a function of Reynolds number. The pressure drop across the impingement system was calculated between the point P_1 and point P_2, which were at $z=1.2$ cm near the nozzle inlet and at $r=4.1$ cm near the tip of the confined plate, respectively. Figures 5(a) and 5(b) show that the small dimensionless channel height, i. e., $H=0.5$, caused a significant increase in the pressure drop more than in the heat transfer coefficient, an observation which is consistent with that reported by Miyazaki and Silberman (1972).

Figure 6(a) presents the local shear stress as a function of dimensionless radial distance for three different dimensionless channel heights for Re= 900 (given here again for reference), whereas Fig. 6(b) shows the corresponding local heat transfer coefficient. The local heat transfer coefficient consistently decreased along the radial direction for $H=1.5$.For $H=0.5$ and 1.0, the local heat transfer coefficient decreased up to a certain radial distance and then increased, reaching a second local maximum value, which might have come from the recirculation flow along the heated bottom plate. From the present results, it is recommended to increase both Reynolds number and the channel height in order to increase heat transfer coefficients without substantially increasing pressure drop.

3.3 Local Nusselt number

3.3.1 Local Nusselt number based on the inlet temperature

Figure 7 presents the local Nusselt numbers as a function of dimensionless radial distance for Reynolds number of 100, 500, and 900. For each Reynolds number case, the local Nusselt number profiles at three different dimensionless channel heights were given. The local Nusselt number was defined as Nu=hd/k, where h is the local heat

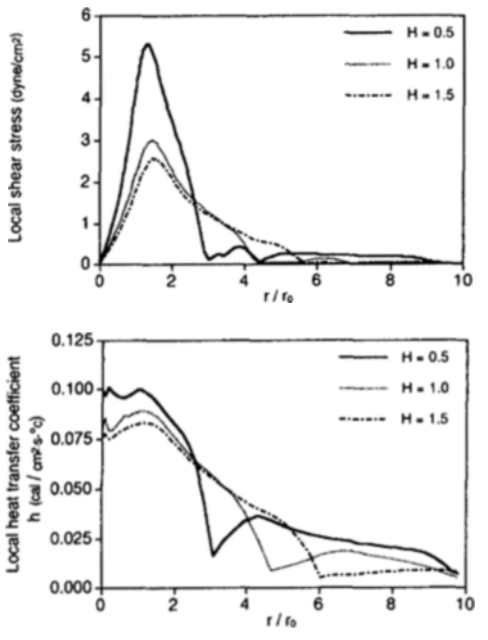

Fig. 6 Shear stress and local heat transfer coefficient distribution along the dimensionless radial distance for $H=0.5$, 1.0 and 1.5 ($Re=900$)

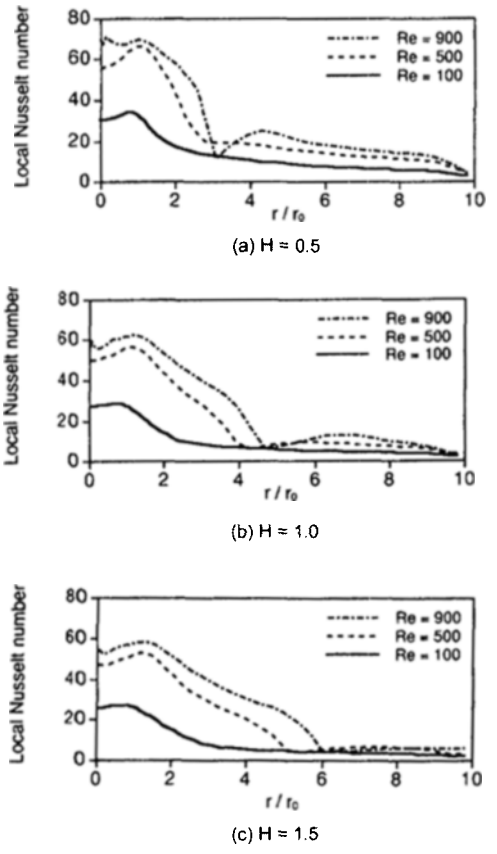

Fig. 7 Nusselt numbers as a function of dimensionless radial distance for $Re=100$, 500 and 1000

transfer coefficient, d is the inner diameter of nozzle, and k is the thermal conductivity of fluid. It is of note that in the calculation of a heat transfer coefficient, one needs to use temperature difference as shown in Eq. (5). In this section, the local heat transfer coefficient was calculated using the temperature difference between the bottom plate temperature T_w and the nozzle inlet temperature T_{in}, which has been used by almost all the previous investigators. Later, however, a new method will be shown to calculate of the local heat transfer coefficient by using the local mixing -cup temperature.

The results in Fig. 7 shows that the local Nusselt number is more sensitive to the Reynolds number than the channel height. Since the local heat transfer coefficient increases with decreasing temperature difference between the bottom plate and the nozzle inlet, the increase in local heat transfer coefficient is magnified as the bottom plate temperature approaches the nozzle inlet temperature. As shown in Fig. 2, the bottom plate temperature was close to the nozzle inlet temperature at the dimensionless radial distance $r/r_0 \leq$ 4.0, resulting in high Nusselt numbers. The Nusselt number did not vary much at $r/r_0 \geq 6.0$ because there was a large temperature difference between the bottom plate and the nozzle inlet.

For $Re=100$, the local Nusselt number reached a peak value at $r/r_0 \cong 1$, and gradually decreased along the radial direction. However, for $Re=900$, the local Nusselt number had generally two peaks as mentioned earlier in Fig. 6(b). The location of the second peak was moving outward radially as the Reynolds number increased and the dimensionless channel height became large. The two peaks were also observed for circular liquid jets in laminar flow by Faghri et al. (1993), in both laminar and turbulent flows by Liu et al. (1991), in turbulent flow by Stevens and Webb (1991), and for circular air jets in turbulent flow by Mohanty and Tawfek (1993) at $r/r_0 \geq 20$. In addition, Sparrow and Wong (1975) also reported this hump in the local Nusselt number profile.

Liu et al. (1991) and Stevens and Webb (1991) considered the second peak as a result of transition from laminar to turbulent flows. Mohanty and Tawfek (1993) regarded the peak as the tendency of the jet to reattach far from the center. Faghri et al. (1993) explained that the wall temperature decreased due to the intersection of two thermal boundary layers forming on the disk. The first boundary layer develops from the jump location and grows downstream. The second boundary layer develops from the end of flow recirculation region and grows upstream due to the direction of the recirculating flow. In this present study, the second peak was attributed to flow recirculation.

Figure 8 presents heat transfer results in the form of $N_{ud}/P_r^{0.4}$ vs. Reynolds number, where the average Nusselt number was defined as Eq (6). Open circles represent the present calculation, whereas open triangles represent the results reported by Womac et al. (1993), who used an unconfined jet impingement. Since most data in Womac et al. were obtained at $Re=2000$, only the average Nusselt numbers for the range of dimensionless distance $r/r_0=2.34$ could be compared under $Re=900$ as shown in Fig. 8. The comparison of these two results indicates that the heat transfer for the present confined jet impingement at $H=1.5$ was slightly larger than that for the unconfined jet impingement (at $H=6.0$). It is of note that the difference in H did not influence the

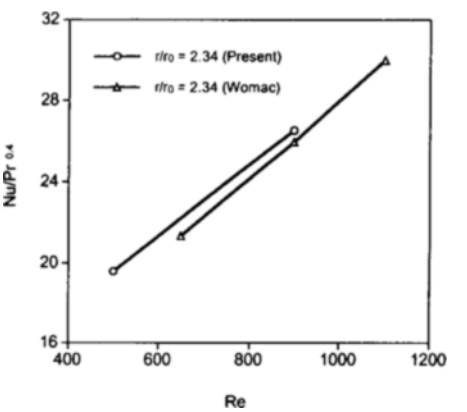

Fig. 8 Comparison of the average Nusselt number between the present results with the confined impingement and Womac et al. (1993) with unconfined impingement under the submerged jet conditions

heat transfer results when the average Nusselt number was computed on a small surface area (i. e., $0 < r/r_0 < 2.34$).

Figure 9 presents the local Nusselt number as a function of dimensionless radial distance for Re= 100, 500 and 900. For each Reynolds number case, Nusselt number profiles at three different channel heights were plotted together with the prediction from Wang et al. (1989) which were obtained from free jet impingement. The comparison of the present confined jet impingement data with Wang's free jet impingement showed that the heat transfer in the confined jet impingement was much larger than that in free jet impingement in the region of $r/r_0 < 4.0$.

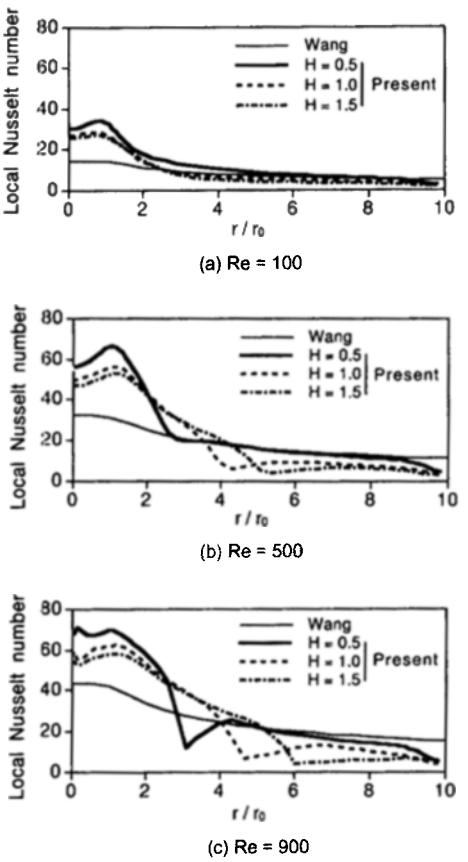

Fig. 9 Comparison of the local Nusselt numbers between the present results with confined impingement and Womac et al. (1993) with unconfined impingement under the submerged jet conditions

3.3.2 Local Nusselt number based on the local mixing-cup temperature

Figure 10 presents the local mixing cup temperature as a function of dimensionless radial distance for three different Reynolds numbers. The inlet temperature was given in dashed line for comparison. The local mixing-cup temperature $T_{mix}(r)$ can numerically be calculated according to the standard definition, which is

$$T_{mix}(r) = \frac{\int TVdA}{A\bar{V}} = \frac{\int TVdA}{\int VdA} \tag{12}$$

Once, $T_{mix}(r)$ is calculated, the local heat transfer coefficient, h_{mix}, can be calculated as follows:

$$q_w = h_{mix}(T_w - T_{mix}) \tag{13}$$

The mixing-cup temperature in the present study was obtained using the concept of energy balance as follow:

$$q_w A = \rho C_p \pi r_0^2 V_{in}(T_{mix} - T_{in}) \tag{14}$$

The right hand side term, $\rho C_p V_{in}(T_{mix} - T_{in})$, represents the energy removed by fluid from the heated bottom plate. It is of note that the mixing-cup temperature does not depend on the channel height because Vin is constant for all H and a given Reynolds number, and the mixing-cup temperature becomes greater at $Re = 100$ than that at

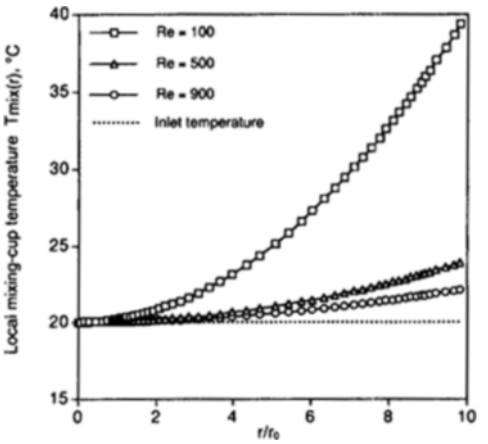

Fig. 10 Local mixing-cup temperature at three different Reynolds numbers. Dashed line, inlet temperature, was provided for comparison

$Re=900$ because the inlet velocity is small for the low Reynolds number.

As mentioned earlier briefly, there are several choices for the fluid temperature used in the calculation of the local heat transfer coefficient. In an external flow, the temperature of the cooling fluid far away from a heated surface is usually known or may be a constant, which justifies the use of the inlet nozzle temperature in the calculation of the local heat transfer coefficient. However, in a confined jet impingement like present study, there is usually no well-defined temperature except the inlet temperature. Hence, the concept of the mixing-cup temperature given in Eq. (12) can be applied.

Figures 11 and 12 present the local Nusselt numbers as a function of dimensionless radial distance for $Re=100$ and 500, respectively. For each Reynolds number case, the local Nusselt number profiles at two different dimensionless channel heights were plotted for both cases using the mixing-cup and the inlet temperatures. The Nusselt number profiles given in these figures show that the local Nusselt numbers calculated using the mixing-cup temperature method were consistently greater than those calculated using the nozzle inlet temperature, although the difference became smaller with increasing Reynolds number. The difference between the two Nusselt numbers also became large with increasing r/r_0. When compared with the temperature difference between the inlet and the heated bottom plate, the temperature difference between local mixing-cup and heated bottom plate decreases along the radial direction because the mixing - cup temperature increases radially as the cooling fluid picks up heat from the bottom plate. Since the heat flux at the bottom plate was constant, the heat transfer coefficients calculated with the mixing-cup temperature method became greater than those calculated with the inlet temperature method.

The results in Figs. 11 and 12 also give the effect of the channel height on the local Nusselt number. The Nusselt numbers for $H=0.5$ was larger than those for $H=1.5$. This is because the mixing-cup temperature does not depend on the channel height while the bottom plate temperature decreases due to high velocity for the small channel height case.

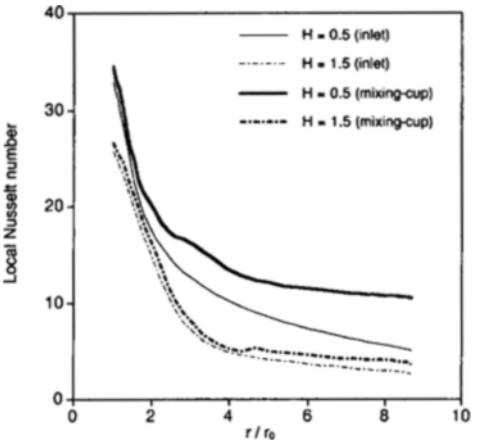

Fig. 11 Comparison of the local Nusselt Numbers calculated using the mixing-cup and inlet temperatures for two different dimensionless channel heights at $Re=100$

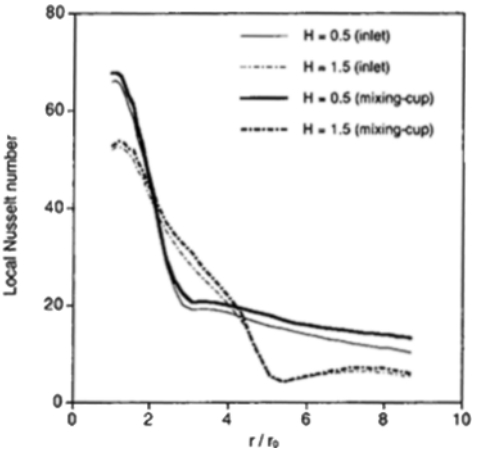

Fig. 12 Comparison of the local Nusselt Numbers calculated using the mixing-cup and inlet temperatures for two different dimensionless channel heights at $Re=500$

As evident in Fig. 10, the mixing-cup temperature is almost identical to the inlet temperature for the case of large Reynolds number, where the convective heat transfer is strong. In this case (i. e., the large Reynolds number case), the local Nusselt numbers calculated using the mixing-cup temperature method are almost the same as those calculated using the inlet temperature method. In

summary, when the Reynolds number is less than 1000, the local Nusselt number should be calculated using the mixing-cup temperature method.

4. Conclusions

The present numerical analysis was carried out to investigate the heat transfer behavior of a steady, axisymmetric, laminar impingement flow with a confinement plate. To examine the effects of both channel height and Reynolds number, three different dimensionless channel heights (H =0.5, 1.0, and 1.5) and three different Reynolds numbers (100, 500 and 900) were used. A brief summary of the present findings is given as follows :

(1) In a confined impingement flow, recirculation zones influencing the local flow and heat transfer behaviors appeared near the confined and the heated bottom plates as Reynolds number and dimensionless channel height increased. Because of these recirculation flows, the bottom plate temperature showed a local maximum value, whereas the local heat transfer coefficient and local Nusselt number curves showed a local minimum value.

(2) Due to the recirculation flow attached to the confined plate, the impingement flow accelerated along the bottom plate near the core area (i. e., $0< r/r_0<5$), resulting in a large variation of the pressure drop and the local wall shear stress. Those were more dependent on the channel height than on the Reynolds number, whereas the local Nusselt number was in the inverse trend. In order to increase the heat transfer coefficients without substantially increasing pressure drop, it is recommended to increase both Reynolds number and channel height (i. e., $Re=900$ and $H=$ 1.5).

(3) Since the mixing-cup temperature, independent on the channel height, became much larger than the inlet temperature for $Re=100$, the local Nusselt number should be calculated using the mixing-cup temperature method in the case of the low Reynolds number.

(4) Since the mixing-cup temperature, independent on the channel height, became much larger than the inlet temperature for $Re=100$, the local Nusselt number should be calculated using the mixing-cup temperature method in the range of low Reynolds number.

(5) Among three dimensionless channel heights (0.5, 1.0 and 1.5) tested, the case of $H=$ 0.5 produced the best heat transfer enhancement due to high velocity. It is also concluded that the local Nusselt number was substantially larger with a confined submerged jet than with an unconfined free jet.

References

Deshpande, M. D. and Vaishnav, R. N., 1982, "Submerged Laminar Jet Impingement on a Plane," *J. Fluid Mech.*, Vol. 114, pp. 213~236.

Downs, S. J. and James, E, H,, 1987, "Jet Impimgement Heat Transfer-a Literature Survey," *Am. Soc. Mech. Eng.*, paper 87-HT-35.

Faghri, A., Thomas, A. and Rahman, M. M., 1993, "Conjugate Heat Transfer From a Disk to a Thin Liquid Film Formed by a Controlled Impinging Jet," *ASME J. of Heat Transfer*, Vol. 115, pp. 116~123.

Inada, S., Miyasaka, Y. and Izumi, R., 1981, "A Study on the Laminar-Flow Heat Transfer between a Two-Dimensional Water Jet and a Flat Surface with Constant Heat Flux," *Bulletin of the JSME*, Vol. 24, pp. 1803~1810.

Liu, X., Lienhard V, J. H. and Lombara, J. S., 1991, "Convective Heat Transfer by Impingement of Circular Liquid Jets," *ASME J. of Heat Transfer*, Vol. 113, pp. 571~582.

Ma, C. F. and Bergles, A. E., 1983, "Boiling Jet Impingement Cooling of Simulated Microelectronic Chips," *in Heat Transfer in Electronic Equipment*, S. Oktay and A. Bar-Cohen, eds., ASME, New York, pp. 5~12.

Miyazaki, H. and Silberman, E., 1972, "Flow and Heat Transfer on a Flat Plate Normal to a Two-Dimensional Laminar Jet Issuing from a Nozzle of Finite Height," *Int. J. Heat Mass Transfer*, Vol. 15, pp. 2097~2107.

Mohanty, A. K. and Tawfek, A. A, 1993, "Heat

Transfer due to a Round Jet Impinging Normal to a Flat Surface," *Int. J. Heat Mass Transfer*, Vol. 36, pp. 1639~1647.

Saad, N. R., Douglas, W. J. M. and Mujumdar, A. S., 1977, "Prediction of Heat Transfer under an Axisymmetric Laminar Impinging Jet," *Ind. Eng. Chem., Fundam.*, Vol. 16, pp. 148~154.

Sparrow, E. M., Xu, Z. X. and Azevedo, L. F. A., 1987, "Heat (Mass) Transfer for Circular Jet Impingement on a Confined Disk with Annular Collection of the Spent Air," *ASME J. of Heat Transfer*, Vol. 109, pp. 329~335.

Stevens, J. and Webb, B. W., 1991, "Local Heat Transfer Coefficients under an Axisymmetric, Single-Phase Liquid Jet," *ASME J. of Heat Transfer*, Vol. 113, pp. 71~77.

Wang, X. S., Dagan, Z. and Jiji, L. M., 1989, "Conjugate Heat Transfer between a Laminar Impinging Liquid Jet and a Solid Disk," *Int. J. Heat Mass Transfer*, Vol. 32, pp. 2189~2197.

Webb, B. W. and Ma, C. F., 1995, "Single -Phase Liquid Jet Impingement Heat Transfer," *Advances in Heat Transfer*, Vol. 26, pp. 105 ~217.

Womac, D. J., Ramadhyani, S. and Incropera, F. P., 1993, "Correlating Equations for Impingement Cooling of Small Heat Sources with Single Circular Liquid Jets," *ASME J. of Heat Transfer*, Vol. 115, pp. 106~115.